HHS Public Access

Author manuscript

Cancer Lett. Author manuscript; available in PMC 2020 February 28.

Published in final edited form as:

Cancer Lett. 2018 December 28; 439: 91–100. doi:10.1016/j.canlet.2018.07.034.

S100B suppression alters polarization of infiltrating myeloid-derived cells in gliomas and inhibits tumor growth

Hang Gao[a,1], **Ian Y. Zhang**[b,1], **Leying Zhang**[b], **Yanyan Song**[c], **Shunan Liu**[d], **Hui Ren**[e], **Huili Liu**[b], **Hui Zhou**[f], **Yanping Su**[g], **Yihang Yang**[h], **Behnam Badie**[i,*]

[a]Department of Bone and Joint Surgery, No.1 Hospital of Jilin University, Changchun, Jilin Province, PR China

[b]Division of Neurosurgery, City of Hope Beckman Research Institute, USA

[c]Department of Nephrology, The Second Hospital of Jilin University, Changchun, Jilin Province, PR China

[d]Department of Pharmacology, The Pharmacy School of Jilin University, Changchun, Jilin Province, PR China

[e]Department of General Surgery, The Second Hospital of Jilin University, Changchun, Jilin Province, PR China

[f]College of Pharmaceutical Sciences, Zhejiang University, Hangzhou, Zhejiang Province, PR China

[g]College of Pharmacy, Fujian Medical University, Fuzhou, Fujian Province, PR China

[h]Department of Neurosurgery, Shandong Provincial Hospital Affiliated to Shandong University, Jinan, Shandong Province, PR China

[i]Department of Cancer Immunotherapeutics & Tumor Immunology, City of Hope Beckman Research Institute, Duarte, CA 91010, USA

Abstract

S100B, a member of the multigene family of Ca^{2+}-binding proteins, is overexpressed by most malignant gliomas but its biological role in gliomagenesis is unclear. Recently, we demonstrated that low concentrations of S100B attenuated microglia activation through the induction of STAT3. Furthermore, S100B downregulation in a murine glioma model inhibited macrophage trafficking and tumor growth. Based on these observations, we hypothesized that S100B inhibitors may have antiglioma properties through modulation of tumor microenvironment.

*Corresponding author. Division of Neurosurgery, City of Hope, 1500 East Duarte Road Duarte, CA, 91010, USA. bbadie@coh.org.

[1]These authors contributed equally to this project.

Conflicts of interest

None.

Appendix A. Supplementary data

Supplementary data related to this article can be found at https://doi.org/10.1016/j.canlet.2018.07.034.

To discover novel S100B inhibitors, we developed a high-throughput screening cell-based S100B promoter-driven luciferase reporter assay. Initial screening of 768 compounds in the NIH library identified 36 hits with >85% S100B inhibitory activity. Duloxetine (Dul, an SNRI) was selected for the initial proof-of-concept studies. At low concentrations (1–5 μM) Dul inhibited S100B and CCL2 production in mouse GL261 glioma cells, but had minimal cytotoxic activity *in vitro*. *In vivo*, however, Dul (30 mg/kg/14 days) inhibited S100B production, altered the polarization and trafficking of tumor-associated myeloid-derived cells, and inhibited the growth of intracranial GL261 gliomas. Dul therapeutic efficacy, however, was not observed in the K-Luc glioma model that expresses low levels of S100B. These findings affirm the role of S100B in gliomagenesis and justify the development of more potent S100B inhibitors for glioma therapy.

Keywords

Brain tumor; Duloxetine; Glioblastoma; Microglia; RAGE; Serotonin-norepinephrine reuptake inhibitor; Tumor-associated macrophages

1. Introduction

Tumor-associated macrophages (TAMs) are heterogeneous cell populations that constitute a major component of inflammatory cells in tumor microenvironment [1]. In gliomas, TAMs are derived in part from CNS microglia and circulating myeloid-derived cells such as monocytes, and have been implicated in glioma angiogenesis, invasion, local tumor recurrence and immunosuppression [2–6]. The mechanisms responsible for the infiltration of TAMs into tumors have been widely studied and inhibition of this process has been proposed as a general treatment strategy for cancer [7]. A variety of cytokines, chemokines and growth factors are involved in TAM trafficking [5,8–12], but CCL2 was the first to be identified in glioma samples [13,14]. Recently we demonstrate that S100B, which is expressed by most gliomas, is an important inducer of CCL2 [15].

S100B is a member of the multigene family of Ca2+-binding proteins which has been implicated in the regulation of cellular activities such as metabolism, motility and proliferation. In the nervous system, S100B is constitutively released by astrocytes into the extracellular space, and at low concentrations (i.e. nM), it's neuroprotective against oxidative stress [16]. S100B expression is also induced by various stimuli such as trauma and inflammation. At high concentrations (i.e. μM), S100B activates microglia and astrocytes in an autocrine fashion through the induction of iNOS and NF-κB, and it increases the expression of pro-inflammatory cytokines. Through these functions, S100B has been implicated in the pathogenesis of brain trauma and neurodegenerative disorders, but its role in gliomagenesis has not been extensively studies.

We recently demonstrated that even at low levels, S100B altered the activity of TAMs in a glioma model by activating STAT3 [17]. We also showed that S100B downregulation in a murine glioma model inhibited TAM trafficking and tumor growth [15]. Based on these findings, we hypothesized that S100B inhibitors may have antiglioma properties through modulation of the tumor microenvironment.

In an effort to discover novel S100B inhibitors in this study, we developed a high-throughput screening (HTS) cell-based S100B promoter-driven luciferase reporter assay. Initial screening of 768 compounds in the NIH library identified 36 hits with > 85% S100B inhibitory activity. One compound, duloxetine (Dul), an FDA-approved serotonin-norepinephrine reuptake inhibitor (SNRI) was selected for the initial proof-of-concept studies. Dul inhibited S100B production in mouse GL261 cell lines, and intracranial (i.c.) GL261 gliomas. Furthermore, Dul shifted TAM polarization into M1-like phenotype and inhibited tumor growth. Dul therapeutic efficacy, however, was not observed in the less immunogenic K-Luc glioma model that expresses low levels of S100B [15]. These observations support the utility of S100B suppression as a novel antiglioma therapy and justify the development of more potent S100B inhibitors.

2. Materials and methods

2.1. Cell lines

Luciferase-expressing GL261 glioma cells (GL261-Luc) were generated as described before [18]. Luciferase-expressing KR158B cells (or KLuc), an invasive glioma cell line that was derived from spontaneous gliomas in *Trp53/Nf1* double-mutant mice in Dr. Tyler Jacks laboratory, was a generous gift from Dr. John Sampson [19]. Both GL261-Luc and K-Luc cells were cultured in DMEM medium supplemented with 10% FBS (BioWhittaker, Walkersville, MD), 100 U/mL penicillin-G, 100 μg/ mL streptomycin and 0.01 M Hepes buffer (Life Technologies, Gaithersburg, MD) in a humidified 5% CO2 atmosphere. Both glioma cell lines were authenticated by short tandem repeat profiling and by histological characterization of i.c. gliomas in mice [20]. Primary astrocytes were generated from newborn pups as described previously [21], cultured in DMEM medium supplemented with 10% FBS, and used 7–10 days later.

2.2. High-throughput screening assay

Luciferase expression vector that is controlled by S100B promoter was purchased from GeneCopoeia (Rockville, MD, #MPRM24745-PG02). This vector was transfected into U251 human gliomas to generate a cell line that expressed luciferase under S100B promoter (U251-Luc). Compounds from the NIH library were screened by using U251-Luc cells in Shared Res-HTS Core-BRI at City of Hope. Briefly, U251-Luc cells (5000/well in 100 μl culture medium) were incubated with each compound serially diluted from a 100 μM stock solution in DMSO. Twenty hours later, gaussia luciferase substrate (100 μl) was added to each well and light emission measured in 20 min by a luminometer (PerkinElmer).

2.3. Cell viability

GL261-Luc cells (5000 cells/96-well plate) were incubated with Dul (0–50 μM) for 24 h prior to the addition of luciferase substrate (100μl/ well). Luciferase activity was measured in a luminometer as a measure of cell viability.

2.4. Duloxetine measurement in tissue

Duloxetine concentrations in tumor tissue and plasma were measured by LC-MS/MS as described by Satonin et al. [22]. Two weeks after GL261 tumor implantation, mice were

given a single dose of Dul (30 mg/kg, oral gavage) and tumors, contralateral brain tissue and plasma were collected for drug level measurements.

2.5. Animals, tumor implantation and duloxetine treatment

All mice were housed and handled in accordance to the approved guidelines of City of Hope Institutional Animal Care and Use Committee under pathogen-free conditions. $CX_3CR_1^{GFP}$ mice that express EGFP under control of the endogenous Cx3cr1 locus were purchased from Jackson Laboratory (Sacramento, CA). Stereotactic intracranial tumor implantation was performed as described before [15]. Briefly, GL261-Luc or K-Luc glioma cells were harvested by trypsinization, counted, and resuspended in culture medium. Female C57BL/6 mice (Jackson Laboratory, Bar Harbor, ME) weighing 15–25 g were anesthetized by intraperitoneal administration of ketamine (132 mg/kg) and xylazine (8.8 mg/kg) and implanted with 10^5 tumor cells using a stereotactic head frame at a depth of 3 mm through a bur hole placed 2 mm lateral and 0.5 mm anterior to the bregma. Dul treatment (5 or 30 mg/kg/day, oral gavage) was initiated one or four days after tumor implantation. Because Dul at either dose caused weight loss after two weeks of oral treatment, therapy was stopped at 14 days for the survival experiments. Thereafter, animals demonstrating signs of elevated intracranial pressure were euthanized and tumor presence confirmed by histology.

2.6. Flow cytometry analysis

Intracranial tumors with peritumoral tissue were harvested and examined by flow cytometry as described previously [15]. Tissue was minced and digested with trypsin for 20 min at 37 °C. The homogenate was then filtered through a 40 μm filter and prepped using Fixation/Permeabilization solution according to the manufacturer's instructions (BD Pharmingen. San Diego, CA). Cells were then incubated with allophycocyanin-conjugated anti-mouse CD11b, PerCP-conjugated anti-mouse CD45, PE-conjugated anti-mouse Ly6C, eFluor 450-conjugated antibody to mouse Ly6G (all 1:100, eBioScience), Pacific Blue-conjugated anti-mouse F4/80 (1:100, Bio-Rad, Irvine, CA), anti-mouse Ly6B (1:100, Bio-Rad) or isotype control antibodies (1 h at 4 °C) prior to FACS analysis. Multiple-color FACS analyses was performed using a 3-laser CyAn immunocytometry system (Dako Cytomation, Fort Collins, CO) and analyzed by FlowJo software (TreeStar, San Carlos, CA). Tumor macrophages were gated as $CD11b^+$ $CD45^{high}$ $F4/80^+$ and microglia as $CD11b^+$ $CD45^{low}$ based on a previously described phenotypic characterization [15,23]. Myeloid-derived suppressive cells were identified as monocytic ($Ly6G^-$ $Ly6C^+$) and granulocytic ($Ly6G^+$ $Ly6C^-$) populations as described previously [24]. Ly6B staining was used to quantify neutrophils.

2.7. Real time RT-PCR, Western blot and ELISA

Real-time quantitative PCR (qPCR) was performed with corresponding primers (Supplementary Table 1) in a TaqMan 5700 Sequence Detection System (Applied Biosystems, Foster City, CA) as described previously [17]. Western blots were performed as describe before [17] using primary antibodies specific for S100B (Abcam), full length RAGE (FL-RAGE, Abcam), CCL2 (Santa Cruse), β-Actin (Abcam) or GAPDH (Cell Signaling). S100B and soluble RAGE (sRAGE) ELISA were performed according to the manufacturer's instructions (MyBioSource).

To assess phenotypes of tumor-associated leukocytes, tumor and peritumoral tissue from control or Dul-treated mice were minced and digestion with trypsin for 20 min at 37 °C. Tissue homogenate was then filtered through a 40 μM filter and leukocytes separated by Percoll gradient (GE Healthcare) at 350 g–400 g for 45 min. The isolated cells were characterized by flow and incubated with LPS (0.5 μg/ml, 24 h) to induce cytokine expression prior to analysis.

2.8. Immunofluorescence staining

Frozen brain sections were prepared from naive and tumor-bearing mice. Immediately after harvest, brains were fixed in paraformaldehyde for 4 h before storage in 30% sucrose solution. Brains were embedded in O.C.T. (Tissue-Tek) and 10 μm sections were cut using a cryostat (Leica Microsystem Inc., Bannockburn, IL). Prior to immunofluorescence staining, slides were baked at 37 °C and permeabilized in methanol for 15 min. Cultured primary astrocytes and GL261 cells were transferred to coverslip slides and permeabilized in methanol for 10 min. After an hour block, slides were incubated with RAGE, S100B (1:300, rabbit anti-mouse, Abcam), CCL2 (1:200, Rabbit anti-mouse, Santa Cruz Biotechnology), NET (1:100 Rabbit anti-mouse, Alomone, Jerusalem, Israel) or GFAP (1:100, Rat anti-mouse, Invitrogen) primary antibodies for 2 h. Slides were washed with PBS three times for 5 min and incubated with secondary antibody (goat anti-rabbit or goat anti-rat Alexa Fluor 594 antibodies (1:200 dilution Thermo Scientific, Waltham, MA) for another hour. Tissue sections were mounted in Vectashield mounting medium containing 4060-diamidino-2-phenylindole (DAPI) (Vector, Burlingame, CA), imaged with AX-70 fluorescent microscopy (Leica Microsystems Inc., Bannockburn, IL) and prepared by Zeiss LSM Image Browser software. Image parameters (i.e. magnification, gain, exposure) were kept constant between each treatment condition. To quantify S100B and RAGE expression, the average number of positive tumor cells per five high-power fields from control and Dul-treated mice were counted (n = 3/group).

2.9. Nanostring analysis

RNA from GL261 and peritumoral brain tissue was extracted using miRNeasy FFPE kit (Qiagen cat# 217504). RNA concentration was assessed with the Nanodrop spectrophotometer ND-1000 and Qubit 3.0 Fluorometer (Thermo Scientific, CA). RNA fragmentation and quality control was determined by 2100 Bioanalyzer (Agilent, CA). RNA expression was analyzed by NanoString nCounter platform (NanoString Technologies, WA) using PanCancer Mouse Immune Profiling panel, which consists of 770 genes covering 24 different immune cell types and populations, and 30 common cancer antigens and genes that represent all categories of immune response. RNA was first hybridized with Codeset from gene panel at 65 °C for 16 h. Post-hybridization probe-target mixture was then purified and quantified with nCounter Digital Analyzer, and all data analysis was performed on nSolver (NanoString Technologies, WA). Pathway Scores were calculated by nSolver Advance Analysis module to summarize the data from a pathway's genes into a single score, using the first principal component (PC) of the expression data [25]. In brief, PC analysis scores each sample using a linear combination of its gene expression values, weighting specific genes to capture the greatest possible variability in the data. The data is presented in a log2 scale. Increased score indicates increased overall expression.

2.10. Statistical analysis

Statistical comparison in all different experimental conditions was performed with the GraphPad Prism software using two-way analysis of variance (ANOVA) or Student's t-test. Survival was plotted using a Kaplan-Meir survival curve and statistical significance was determined by the Log-rank (Mantel-Cox) test. A P value of less than 0.05 was considered significant.

3. Results

3.1. S100B inhibitor screening assay

To discover novel S100B inhibitors, we developed a HTS cell-based S100B promoter-driven luciferase reporter assay in the human U251 glioma cell line that expresses S100B. Initial screening of 768 compounds in the NIH library identified 36 hits with > 85% S100B inhibitory activity. One compound, Dul, an FDA-approved SNRI, was selected for the initial proof-of-concept studies because of its potency and low toxicity profile, and because it is currently in clinical use for a variety of neurological disorders.

3.2. Duloxetine inhibits S100B expression in GL261 gliomas

At 5 μM, (concentration below the IC_{50} of 10 μM), Dul inhibited S100B promoter activity in U251 glioma cells (Fig. 1A) without causing cytotoxicity in either U251 (not shown) or mouse GL261 gliomas (Fig. 1B). At low concentrations, Dul also inhibited S100B expression as measured by qPCR, Western analysis, ELISA and immunostains of GL261 cells. (Fig. 1C). Dul also inhibited CCL2 expression by GL261 cells (Fig. 1D). *In vivo*, however, neither low (5 mg/kg/14 days) nor high (30 mg/kg/14 days) doses of Dul inhibited S100B, CCL2 or RAGE (S100B receptor) protein levels in i.c GL261 gliomas (Fig. 2A). Nor mouse serum S100B and soluble RAGE (sRAGE) levels changed after Dul therapy (Fig. 2B). To explore this lack of *in vivo* S100B-inhibitory activity, we then measured Dul concentrations in mice bearing i.c. GL261 gliomas. Two weeks after GL261 tumor implantation, mice were given a single dose of Dul (30 mg/kg, oral gavage) and tumors, contralateral brain tissue and plasma were collected for drug level measurement with LC-MS/MS (Table 1). These studies confirmed that Dul did indeed penetrate into both the brain and i.c. GL261 tumors within an hour of administration, and remained at therapeutic levels (i.e. > 10 μM) for up to 12 h. Thus, its inability to suppress S100B *in vivo* was not due to CNS penetration.

To further evaluate the *in vivo* Dul activity, histochemistry was used to measure the expression of S100B in i.c. GL261 tumors. Interestingly, Dul effectively inhibited S100B and RAGE (S100B receptor) in tumors, but not in the peritumoral brain (Fig. 2C). Further analysis of the brains from Dul-treated mice showed that most of the $S100B^+$ cells were $GFAP^+$ astrocytes that surrounded the tumor margin (Fig. 2D). These observations confirmed that whereas Dul had good CNS penetration and effectively inhibited S100B in GL261 gliomas, it had minimal impact on the production of S100B by peritumoral reactive astrocytes.

As an SNRI, Dul's mechanism of action occurs through inhibition of the norepinephrine (NE) transporter (NET) in neurons. Because GL261 gliomas have been shown to express monoamine receptors [26], we hypothesized that lack of S100B inhibition in normal astrocytes was due to absence of NET in normal astrocytes. Indeed, GL261, but not astrocytes, were positive for NET *in vitro* (Fig. 3A) and in i.c. GL261 tumors (Fig. 3B). Furthermore, NE induced the expression of S100B in GL261 (Fig. 3C), and S100B promoter activity in U251-Luc human gliomas (Fig. 3D). Induction of S100B by NE was also partially inhibited by Dul (Fig. 3B). These observations suggest that Dul suppression of S100B in GL261 tumors (but not reactive astrocytes) was most likely mediated by inhibition of NE uptake by tumor cells.

3.3. Duloxetine attenuates the growth of intracranial GL261 gliomas

To test the effect of Dul on tumor growth, mice were implanted with i.c. GL261 cells and then treated with Dul for 14 days. When treatment was initiated a day after tumor implantation, tumor growth significantly decreased (Fig. 4A) and animal survival improved with high doses of Dul (Fig. 4B). However, neither low nor high doses of Dul had any survival benefit when the 14-day treatment was started four days after tumor implantation when tumors were larger and already infiltrated by TAMs (Supplemental Fig. 1). These observations, combined with lack of direct *in vitro* inhibitory effect on GL261 gliomas (Fig. 1B), suggested that the antitumor activity of Dul was most likely due to alteration of tumor microenvironment and not direct tumor cytotoxicity.

3.4. Duloxetine alters TAM trafficking and polarization

We previously reported that S100B stimulates CCL2 expression and enhances TAM infiltration into GL261 gliomas. Because Dul inhibited S100B production by tumors (but not tumor-associated astrocytes) we next evaluated its effect on tumor inflammatory responses. To assess the overall inflammatory changes in tumor and TME, tumors and peritumoral tissue from brains of control and Dul-treated GL261-bearing mice were dissected and analyzed by Nanostring (Fig. 5A). Interestingly, Pathway Scores for a number of processes involved in innate and adaptive immunity were significantly higher in Dul-treated tumors, but not in the TME. Furthermore, treatment with Dul decreased the proportion of macrophages (i.e. $CD11b^{+}$ $CD45^{high}$ $F4/80^{+}$), monocytic myeloid-derived cells ($CD11b^{+}$ $Ly6G^{-}$ $Ly6G^{+}$) and neutrophils ($Ly6B^{+}$), but not microglia (i.e. $CD11b^{+}$ $CD45^{low}$) in GL261 gliomas (Fig. 5B). In addition, trafficking pattern of inflammatory cells appeared to be different in Dul-treated animals; fewer cells infiltrated the tumor mass itself while inflammatory cell infiltration around the tumors (probably microglia) was more prominent in the Dul-treated animals (Fig. 5C). Finally, a reduction in the infiltration of inflammatory cells into the tumor mass also correlated with a decrease in CCL2 expression in GL261 gliomas (Fig. 5D). In summary, although the Pathway Scores for inflammatory processes was higher in Dul-treated tumors, the infiltration of TAMs appeared to be suppressed in the tumor mass itself.

To assess changes in TAM polarization, cytokine expression was also evaluated in tumor-associated leukocytes. Inflammatory cells isolated from GL261 gliomas, which mostly consisted of monocytic lineage (i.e. microglia, macrophages and monocytic myeloid-derived

cells) (Fig. 5E) expressed higher levels of pro-inflammatory cytokine *Il-1β*, but lower levels of *Il-6*, *Il-10* and *Tgf-β* (M2 cytokines) after Dul therapy (Fig. 5F).

3.5. Duloxetine antitumor response was dependent on S00B production

To evaluate the effect of Dul on a different syngeneic glioma model, we next studied the K-Luc cell line that expresses lower levels of S100B [15]. Dul had modest inhibitory effect on cell proliferation *in vitro* (Fig. 6A), but similar to the GL261 model, it did not significantly change the overall tumor levels of S100B and RAGE (Fig. 6B). Expression of S100B by peritumoral astrocytes ($GFAP^+$), however, appeared to be slightly higher in Dul-treated mice (Fig. 6C). But, in contrast to the GL261 model, a two-week treatment with Dul did not significantly inhibit the growth of K-Luc tumors (Fig. 6D).

4. Discussion

In glioma microenvironment, TAMs may be polarized to promote tumor growth, angiogenesis and invasion [1]. Although a number of factors can alter TAM immune function, the role of S100B has not been investigated in detail. Building on our previous observations that S100B activates STAT3 in microglia, and enhances TAM infiltration into gliomas, we hypothesized that S100B inhibitors could potentially alter TAM innate immune function in brain tumors. Here, Dul was identified as an inhibitor of S100B promoter activity in a human glioma cell line. Although Dul had minimal *in vitro* cytotoxicity at low doses, it inhibited the growth of GL261 gliomas (which express high levels of S100B) by inhibiting the infiltration of TAMs and by shifting the polarization of myeloid-derived cells into pro-inflammatory subtypes. Interestingly, this biological function was not seen in the K-Luc glioma model that expresses low levels of S100B. To our knowledge, this is the first report demonstrating the role of Dul, a SNRI, as an immune modulator in gliomas.

Anti-neoplastic activity of antidepressants has been reported previously. Epidemiologic studies have suggested a significantly reduced risk of colorectal cancer among users of high doses of selective serotonin reuptake inhibitors (SSRIs) [27]. Furthermore, various SSRIs have demonstrated apoptotic activity in different cancer cell types and even inhibit growth of human cancer xenografts in mice [28]. SSRIs can also inhibit glioma proliferation *in vitro* (at concentrations above 5 μM) and have synergistic effects with imatinib (a multi tyrosine kinase inhibitor) by decreasing AKT phosporylation [29–31]. In our study, however, the antitumor activity of Dul was most likely independent of its direct cytotoxicity, but rather, due to its modulation of the TME. First, *in vitro* tumoricidal activity of Dul occurred at high concentrations (above 20 μM), while it inhibited CCL2 expression at lower levels (i.e. 1–2.5 μM). Second, antitumor efficacy of Dul was not seen if the two-week treatment was initiated four days after tumor implantation, possibly because TAMs begin to infiltrate i.c. gliomas within a few days of implantation and initiate a cascade of events that attract other inflammatory cells [32]. Others have also shown CCL2 to play a critical role in tumor initiation, but not tumor progression [33]. If Dul antitumor activity was exclusively due to its tumor cytotoxicity, then delayed therapy should have also abrogated the growth of larger tumors. Finally, *in vivo* antitumor activity of Dul was dependent on the expression of S100B by the tumor. Although K-Luc proliferation was partially inhibited by Dul *in vitro*, in

contrast to the GL261 gliomas, these low S100B-producing tumors did not respond to Dul therapy in vivo. Thus, Dul antitumor response in the GL261 gliomas was likely due to its modulation of TME through S100B inhibition, and not its direct tumoricidal activity.

We previously reported that upregulation of CCL2 by S100B in gliomas promoted TAM recruitment [15]. Consistent with this observation, in the current study, Dul inhibited S100B and CCL2 production by GL261 gliomas, and prevented TAM infiltration into tumor mass. However, changes in TAM trafficking appeared to vary for each $CD11b^+$ subpopulation. Whereas Dul inhibited macrophage ($CD11b^+$, $CD45^{high}$, $F4/80^+$) infiltration into the tumors, recruitment of other $CD11b^+$ cells into tumor edge was not significantly altered. We speculate that the peritumoral TAMs mostly originated from CNS microglia, and unlike macrophages, their proportion did not significantly change after Dul therapy. Furthermore, these cells accumulated around the tumor margin, and not in the tumor mass itself. Using chimeric mice, we recently showed that most microglia are located around the tumor edge, in contrast to the macrophages which infiltrate into the GL261 gliomas [20]. Therefore, despite inhibition of S100B and CCL2, microglia (and perhaps other $Ly6G^+$ myeloid-derived cells) still persisted around GL261 tumor margin, possibly due to the expression of chemokines/cytokines by peritumoral $S100B^+$ reactive astrocytes.

Besides altering leukocyte trafficking, Dul also promoted the polarization of TAMs into M1-like macrophages. TAMs in Dul-treated GL261 gliomas expressed higher levels of IL-1β, but lower levels of IL-6, IL-10 and TGF-β. Although TAM subpopulations (i.e. microglia and macrophages) were not investigated separately, these findings suggest an overall shift in TAM polarization into pro-inflammatory phenotype after Dul therapy. S100B has diverse biological functions, and at low concentrations, it activates STAT3 in TAMs [17]. Thus, TAM polarization into M1 phenotype could have been due to the inhibition of STAT3 pathway. Alternatively, Dul could have directly activated TAMs by increasing the concentrations of serotonin and S100B in the peritumoral tissue. Although Dul suppressed S100B production by GL261, it did not inhibit S100B in peritumoral astrocytes. Others have shown serotonin (via $5HT_{1A}$-R) to stimulate S100B secretion by astrocytes [34]. Furthermore, fluoxetine, another SSRI, stimulated S100B expression in rat astrocytes in vivo [35]. Therefore, in contrast to its inhibition of S100B in GL261 gliomas, Dul may have stimulated the secretion of S100B by reactive astrocytes in the TME. Because S100B has pro-inflammatory functions at μM concentrations, higher peritumoral S100B levels may have induced IL-1β expression by peritumoral microglia and other myeloid-derived cells.

The mechanism by which Dul inhibited S100B expression in gliomas, but not in the peritumoral astrocytes, is unclear. Our observations suggest this incongruent response to Dul to be due to variations in NET expression. GL261 cells expressed higher levels of NET and upregulated S100B expression after NE exposure. These findings are consistent with other reports that showed higher monoamine transporters expression by i.c. GL261 gliomas [26]. Similarly, Tsoporis et al. demonstrated NE to be an inducer of S100B expression in cardiac myocytes [36]. Therefore, by inhibiting NE uptake, Dul selectively inhibited the expression of S100B in GL261 cells but not astrocytes that expressed lower levels of NET. However, the exact mechanism by which NE induces S100B in glioma cells was not explored here. S100B promoter has binding sites for a number of regulatory elements (such as NF-κB,

AP-1, STAT1 and p53). Others have shown intracellular NE to activate NF-κB, AP-1 and Stat transcription factors [37,38]. Thus, alterations of these regulatory pathways by NE could have influenced S100B expression by gliomas.

In addition to modulating TAM activity, Dul could have simulated other immune cells by increasing serotonin levels in the TME. T, B and NK cells express serotonin, dopamine and norepinephrine receptors and are potential targets for SSRIs. NK cell activity, for example, can increase with fluoxetine and paoxetine [39]. Frick et al. have also reported fluoxetine to increase IFN-γ and TNF-α expression, and to inhibit lymphoma growth through the modulation of T cell responses at similar doses studied here [40,41]. The effect of Dul on other leukocytes was not studied here, therefore, we cannot exclude their role in Dul's antitumor activity.

In summary, we have identified Dul as an S100B inhibitor in GL261 gliomas, and demonstrated its ability to shift TAM polarization into pro-inflammatory subtypes. Although direct tumoricidal activity of Dul was modest, its impact on TME could be exploited to enhance immunemediated therapies against malignant gliomas. For example, by shifting the immune-suppressive TME into an immune-permissive one, Dul (or other S100B inhibitors) could potentially enhance cytotoxic T cell penetration into gliomas. Our Future studies will screen other S100B inhibitors on both gliomas and normal astrocytes, and evaluate their antitumor efficacy in combination with immunotherapy approaches.

Supplementary Material

Refer to Web version on PubMed Central for supplementary material.

Acknowledgements

We thank Timothy Synold for assisting with LC-MS/MS measurements of Dul concentrations, and Holly Yin and Raju K. Pillai for Nanostring tissue analysis.

Funding

Research reported in this publication was supported by the National Cancer Institute and National Institute of Neurological Disorders and Stroke of the National Institutes of Health (R01CA155769, R21NS081594, R21CA189223 and P30CA33572).

Research reported in this publication included work performed in the Analytical Cytometry, Analytical Pharmacology and Molecular Pathology Cores supported by the National Cancer Institute of the National Institutes of Health under award number P30CA033572. The content is solely the responsibility of the authors and does not necessarily represent the official views of the National Institutes of Health.

Abbreviations

Dul	Duloxetine
HTS	High-throughput screening
i.c.	Intracranial
RAGE	Receptor for advanced glycation endproducts

SNRI	Serotonin-norepinephrine reuptake inhibitor
SSRI	Selective serotonin reuptake inhibitors
STAT3	Signal tranducer and activator of transcription 3
TAMs	Tumor-associated macrophages
TME	Tumor microenvironment

References

[1]. Mantovani A, Sica A, Macrophages, innate immunity and cancer: balance, tolerance, and diversity, Curr. Opin. Immunol 22 (2010) 231–237. [PubMed: 20144856]

[2]. Du R, Lu KV, Petritsch C, Liu P, Ganss R, Passegué E, Song H, VandenBerg S, Johnson RS, Werb Z, Bergers G, HIF1α induces the recruitment of bone marrowderived vascular modulatory cells to regulate tumor angiogenesis and invasion, Canc. Cell 13 (2008) 206–220.

[3]. Gabrusiewicz K, Rodriguez B, Wei J, Hashimoto Y, Healy LM, Maiti SN, Thomas G, Zhou S, Wang Q, Elakkad A, Liebelt BD, Yaghi NK, Ezhilarasan R, Huang N, Weinberg JS, Prabhu SS, Rao G, Sawaya R, Langford LA, Bruner JM, Fuller GN, Bar-Or A, Li W, Colen RR, Curran MA, Bhat KP, Antel JP, Cooper LJ, Sulman EP, Heimberger AB, Glioblastoma-infiltrated innate immune cells resemble M0 macrophage phenotype, JCI insight 1 (2016).

[4]. Raychaudhuri B, Rayman P, Ireland J, Ko J, Rini B, Borden EC, Garcia J, Vogelbaum MA, Finke J, Myeloid-derived suppressor cell accumulation and function in patients with newly diagnosed glioblastoma, Neuro Oncol. 13 (2011) 591–599. [PubMed: 21636707]

[5]. Wang SC, Hong JH, Hsueh C, Chiang CS, Tumor-secreted SDF-1 promotes glioma invasiveness and TAM tropism toward hypoxia in a murine astrocytoma model, Lab. Invest 92 (2012) 151–162. [PubMed: 21894147]

[6]. Zhai H, Heppner FL, Tsirka SE, Microglia/macrophages promote glioma progression, Glia 59 (2011) 472–485. [PubMed: 21264953]

[7]. Lazennec G, Richmond A, Chemokines and chemokine receptors: new insights into cancer-related inflammation, Trends Mol. Med 16 (2010) 133–144. [PubMed: 20163989]

[8]. Kerber M, Reiss Y, Wickersheim A, Jugold M, Kiessling F, Heil M, Tchaikovski V, Waltenberger J, Shibuya M, Plate KH, Machein MR, Flt-1 signaling in macrophages promotes glioma growth in vivo, Canc. Res 68 (2008) 7342–7351.

[9]. Held-Feindt J, Hattermann K, Muerkoster SS, Wedderkopp H, Knerlich-Lukoschus F, Ungefroren H, Mehdorn HM, Mentlein R, CX3CR1 promotes recruitment of human glioma-infiltrating microglia/macrophages (GIMs), Exp. Cell Res 316 (2010) 1553–1566. [PubMed: 20184883]

[10]. Hao C, Parney IF, Roa WH, Turner J, Petruk KC, Ramsay DA, Cytokine and cytokine receptor mRNA expression in human glioblastomas: evidence of Th1, Th2 and Th3 cytokine dysregulation, Acta Neuropathol. 103 (2002) 171–178. [PubMed: 11810184]

[11]. Coniglio SJ, Eugenin E, Dobrenis K, Stanley ER, West BL, Symons MH, Segall JE, Microglial stimulation of glioblastoma invasion involves epidermal growth factor receptor (EGFR) and colony stimulating factor 1 receptor (CSF-1R) signaling, Mol. Med 18 (2012) 519–527. [PubMed: 22294205]

[12]. Badie B, Schartner J, Klaver J, Vorpahl J, In vitro modulation of microglia motility by glioma cells is mediated by hepatocyte growth factor/scatter factor, Neurosurgery 44 (1999) 1077–1082; discussion 1082–1073. [PubMed: 10232541]

[13]. Leung SY, Wong MP, Chung LP, Chan AS, Yuen ST, Monocyte chemoattractant protein-1 expression and macrophage infiltration in gliomas, Acta Neuropathol. 93 (1997) 518–527. [PubMed: 9144591]

[14]. Desbaillets I, Tada M, de Tribolet N, Diserens AC, Hamou MF, Van Meir EG, Human astrocytomas and glioblastomas express monocyte chemoattractant protein-1 (MCP-1) in vivo and in vitro, Int. J. Canc 58 (1994) 240–247.

[15]. Wang H, Zhang L, Zhang IY, Chen X, Da Fonseca A, Wu S, Ren H, Badie S, Sadeghi S, Ouyang M, Warden CD, Badie B, S100B promotes glioma growth through chemoattraction of myeloid-derived macrophages, Clin. Canc. Res 19 (2013) 3764–3775.

[16]. Donato R, Intracellular and extracellular roles of S100 proteins, Microsc. Res. Tech 60 (2003) 540–551. [PubMed: 12645002]

[17]. Zhang L, Liu W, Alizadeh D, Zhao D, Farrukh O, Lin J, Badie SA, Badie B, S100B attenuates microglia activation in gliomas: possible role of STAT3 pathway, Glia 59 (2011) 486–498. [PubMed: 21264954]

[18]. Alizadeh D, Zhang L, Brown CE, Farrukh O, Jensen MC, Badie B, Induction of anti-glioma natural killer cell response following multiple low-dose intracerebral CpG therapy, Clin. Canc. Res 16 (2010) 3399–3408.

[19]. Terada K, Wakimoto H, Tyminski E, Chiocca EA, Saeki Y, Development of a rapid method to generate multiple oncolytic HSV vectors and their in vivo evaluation using syngeneic mouse tumor models, Gene Ther. 13 (2006) 705–714. [PubMed: 16421599]

[20]. Chen X, Zhang L, Zhang IY, Liang J, Wang H, Ouyang M, Wu S, da Fonseca AC, Weng L, Yamamoto Y, Yamamoto H, Natarajan R, Badie B, RAGE expression in tumor-associated macrophages promotes angiogenesis in glioma, Canc. Res. 74 (2014) 7285–7297.

[21]. Lian H, Roy E, Zheng H, Protocol for primary microglial culture preparation, Bio Protoc 6 (2016).

[22]. Satonin DK, McCulloch JD, Kuo F, Knadler MP, Development and validation of a liquid chromatography-tandem mass spectrometric method for the determination of the major metabolites of duloxetine in human plasma, J Chromatogr B Analyt Technol Biomed Life Sci 852 (2007) 582–589.

[23]. Badie B, Schartner JM, Flow cytometric characterization of tumor-associated macrophages in experimental gliomas, Neurosurgery 46 (2000) 957–961; discussion 961–952. [PubMed: 10764271]

[24]. Fan H, Zhang I, Chen X, Zhang L, Wang H, Da Fonseca A, Manuel ER, Diamond DJ, Raubitschek A, Badie B, Intracerebral CpG immunotherapy with carbon nanotubes abrogates growth of subcutaneous melanomas in mice, Clin. Canc. Res 18 (2012) 5628–5638.

[25]. Tomfohr J, Lu J, Kepler TB, Pathway level analysis of gene expression using singular value decomposition, BMC Bioinf. 6 (2005) 225.

[26]. Kucheryavykh LY, Kucheryavykh YV, Rolon-Reyes K, Skatchkov SN, Eaton MJ, Cubano LA, Inyushin M, Visualization of implanted GL261 glioma cells in living mouse brain slices using fluorescent 4-(4-(dimethylamino)-styryl)-N-methylpyridinium iodide (ASP+), Biotechniques 53 (2012) 305–309. [PubMed: 23570046]

[27]. Xu W, Tamim H, Shapiro S, Stang MR, Collet J-P, Use of antidepressants and risk of colorectal cancer: a nested case-control study, Lancet Oncol. 7 (2006) 301–308. [PubMed: 16574545]

[28]. Stepulak A, Rzeski W, Sifringer M, Brocke K, Gratopp A, Kupisz K, Turski L, Ikonomidou C, Fluoxetine inhibits the extracellular signal regulated kinase pathway and suppresses growth of cancer cells, Canc. Biol. Ther 7 (2008) 1685–1693.

[29]. Tzadok S, Beery E, Israeli M, Uziel O, Lahav M, Fenig E, Gil-Ad I, Weizman A, Nordenberg J, In vitro novel combinations of psychotropics and anti-cancer modalities in U87 human glioblastoma cells, Int. J. Oncol 37 (2010) 1043–1051. [PubMed: 20811727]

[30]. Spanova A, Kovaru H, Lisa V, Lukasova E, Rittich B, Estimation of apoptosis in C6 glioma cells treated with antidepressants, Physiol. Res 46 (1997) 161–164. [PubMed: 9727508]

[31]. Levkovitz Y, Gil-Ad I, Zeldich E, Dayag M, Weizman A, Differential induction of apoptosis by antidepressants in glioma and neuroblastoma cell lines, J. Mol. Neurosci 27 (2005) 29–42. [PubMed: 16055945]

[32]. Chang AL, Miska J, Wainwright DA, Dey M, Rivetta CV, Yu D, Kanojia D, Pituch KC, Qiao J, Pytel P, Han Y, Wu M, Zhang L, Horbinski CM, Ahmed AU, Lesniak MS, CCL2 produced by the glioma microenvironment is essential for the recruitment of regulatory T cells and myeloid-derived suppressor cells, Canc. Res 76 (2016) 5671–5682.

[33]. Feng X, Szulzewsky F, Yerevanian A, Chen Z, Heinzmann D, Rasmussen RD, Alvarez-Garcia V, Kim Y, Wang B, Tamagno I, Zhou H, Li X, Kettenmann H, Ransohoff RM,

Hambardzumyan D, Loss of CX3CR1 increases accumulation of inflammatory monocytes and promotes gliomagenesis, Oncotarget 6 (2015) 15077–15094. [PubMed: 25987130]

[34]. Whitaker-Azmitia PM, Murphy R, Azmitia EC, Stimulation of astroglial 5-HT1A receptors releases the serotonergic growth factor, protein S-100, and alters astroglial morphology, Brain Res. 528 (1990) 155–158. [PubMed: 2245332]

[35]. Bock N, Koc E, Alter H, Roessner V, Becker A, Rothenberger A, Manzke T, Chronic fluoxetine treatment changes S100B expression during postnatal rat brain development, J. Child Adolesc. Psychopharmacol 23 (2013) 481–489. [PubMed: 24024533]

[36]. Tsoporis JN, Marks A, Van Eldik LJ, O'Hanlon D, Parker TG, Regulation of the S100B gene by alpha 1-adrenergic stimulation in cardiac myocytes, Am. J. Physiol. Heart Circ. Physiol 284 (2003) H193–H203. [PubMed: 12388300]

[37]. Villela D, de Sa Lima L, Peres R, Peliciari-Garcia RA, do Amaral FG, Cipolla-Neto J, Scavone C, Afeche SC, Norepinephrine activates NF-kappaB transcription factor in cultured rat pineal gland, Life Sci. 94 (2014) 122–129. [PubMed: 24239639]

[38]. Zhong H, Lee D, Robeva A, Minneman KP, Signaling pathways activated by alpha1-adrenergic receptor subtypes in PC12 cells, Life Sci. 68 (2001) 2269–2276. [PubMed: 11358336]

[39]. Frank MG, Hendricks SE, Johnson DR, Wieseler JL, Burke WJ, Antidepressants augment natural killer cell activity: in vivo and in vitro, Neuropsychobiology 39 (1999) 18–24. [PubMed: 9892855]

[40]. Frick LR, Rapanelli M, Arcos MLB, Cremaschi GA, Genaro AM, Oral administration of fluoxetine alters the proliferation/apoptosis balance of lymphoma cells and up-regulates T cell immunity in tumor-bearing mice, Eur. J. Pharmacol 659 (2011) 265–272. [PubMed: 21497159]

[41]. Frick LR, Palumbo ML, Zappia MP, Brocco MA, Cremaschi GA, Genaro AM, Inhibitory effect of fluoxetine on lymphoma growth through the modulation of antitumor T-cell response by serotonin-dependent and independent mechanisms, Biochem. Pharmacol 75 (2008) 1817–1826. [PubMed: 18342838]

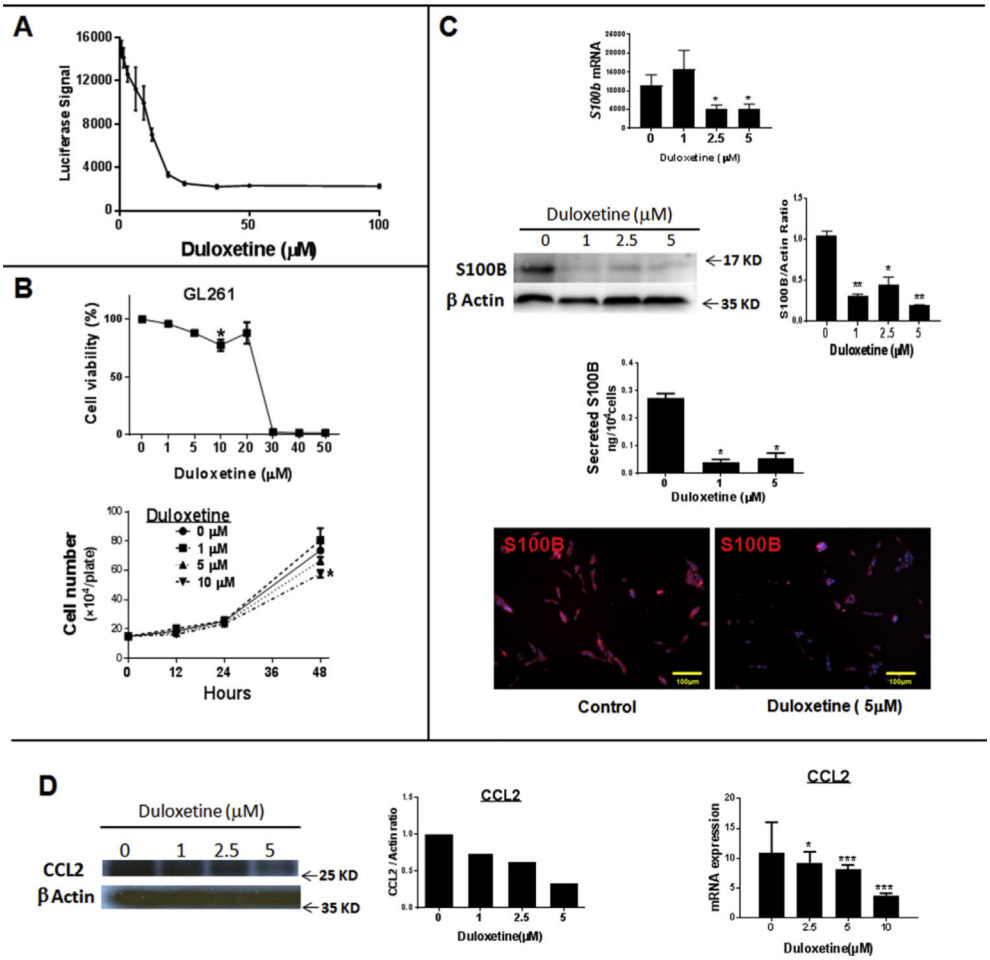

Fig. 1. Duloxetine (Dul) inhibits S100B expression *In vitro*.

(A) Dul inhibition of S100B promoter activity by a luciferase reporter assay in the human U251 glioma cell line. Luciferase activity was measured 24 h after Dul treatment. n= 3 ± SD **(B)** Dul cytotoxicity in GL261 glioma cell line. GL261-Luc cells were incubated with Dul for 24 h before measuring luciferase activity per plate (upper panel); LD50 = 25.1 μM. Cell proliferation was not significantly inhibited at Dul at concentration < 10 μM (lower panel). n = 3 ± SD, *: $p < 0.05$ compared to control. (C) Inhibition of S100B expression by GL261 cells after 24 h (qPCR, top panel) and 48 h (Western analysis, ELISA and immunostains) incubations with Dul. n = 3 ± SD. **(D)** *In vitro* inhibition of CCL2 protein (left panels) and RNA expression (right panel) in GL261 cells after a 48 h incubation with Dul. n = 5 ± SD. *: $p < 0.05$, **: $p < 0.01$, ***: $p < 0.001$. Experimental results are representative of at least two separate experiments.

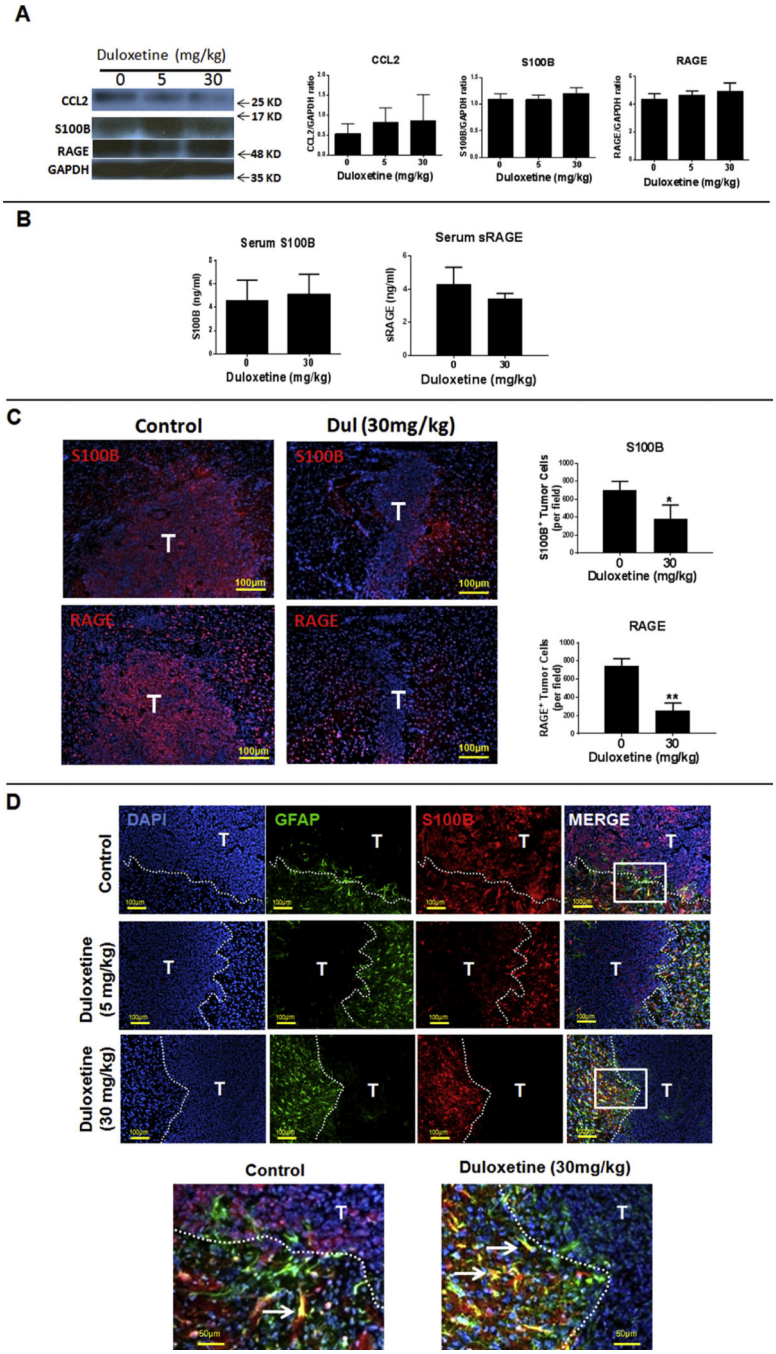

Fig. 2. ***In vivo*** **activity of Duloxetine (Dul) in the mouse intracranial (i.c.) GL261 glioma model.** **(A)** Dul did not significantly inhibit total brain S100B, RAGE or CCL2 protein levels in tumor-bearing animals. One day after tumor implantation, tumor-bearing mice (n = 3) were treated daily with different doses of Dul or vehicle. Fourteen days later, tumors and peritumoral tissue was harvested for protein analysis. **(B)** Serum levels of S100B and soluble RAGE (sRAGE) of tumor-bearing mice with and without a two-week treatment with Dul. n = 5–6 mice/group ± SD. **(C)** Representative immunostains of i.c. GL261 tumors (T, left panels) following a two-week treatment with Dul demonstrating significant inhibition of

S100B and RAGE-positive tumor cells (bar graphs). n = 3 mice/ group ± SD. *: $p < 0.05$, **: $p < 0.01$. **(D)** Effect of Dul therapy on the expression of S100B by i.c. GL261 tumors (T) and peritumoral reactive astrocytes ($GFAP^+$ cells). Low (top panels) and high magnification (lowest panel) of tumor sections demonstrating effective inhibition of S100B by tumors, but not by peritumoral reactive astrocytes (arrows). GFAP: glial fibrillary acidic protein. Representative results from two separate experiments is shown.

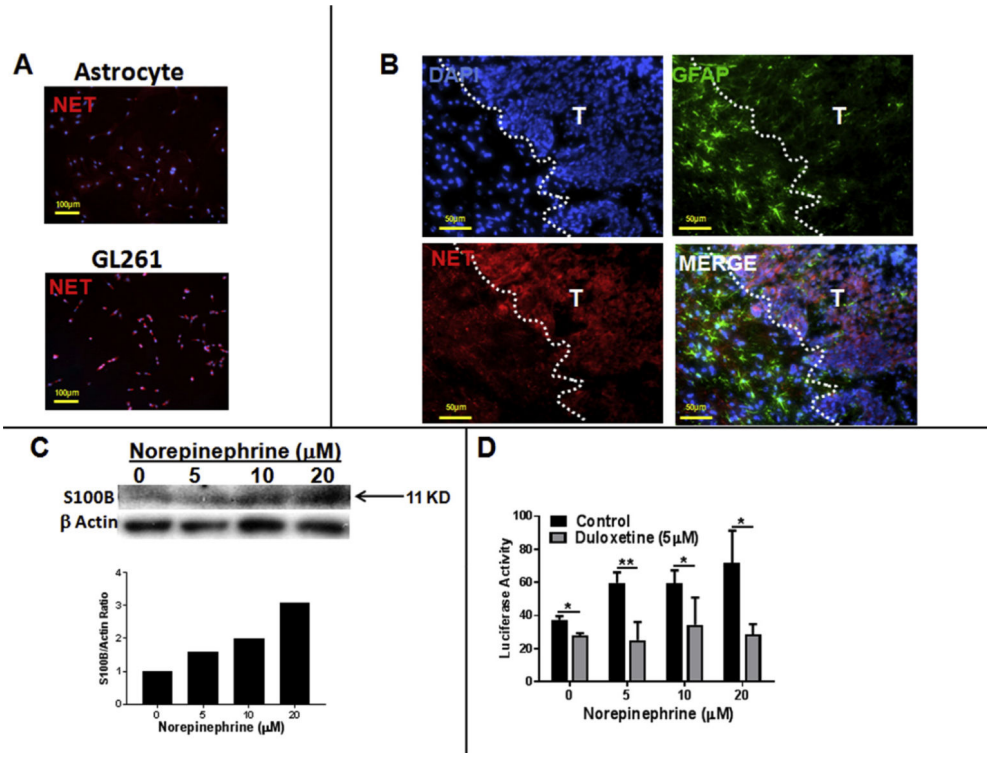

Fig. 3. S100B expression in gliomas is enhanced by norepinephrine (NE).

(A) Norepinephrine transporter (NET) is expressed by GL261 glioma, but not by primary astrocytes. **(B)** In vivo expression of NET in i.c. GL261 gliomas (T) but not peritumoral astrocytes ($GFAP^+$ cells). **(C)** Expression of S100B by GL261 cells is induced by NE. Cells (4×10^5 cells/plate) were treated with NE every 3 h. After 24 h, cells were lysed and subjected to Western analysis. **(D)** Inhibition of S100B promoter activity by Dul. U251 human gliomas (5000 cell/plate) that were stably transfected with S100B reporter gene were incubated with NE (added every 3 h to the medium) in presence and absence of Dul (5 μM). Luciferase activity was measured in 12 h n = 3/group ± SD. *: $p < 0.05$, **: $p < 0.01$ compared to control group. Representative results from two separate experiments is shown.

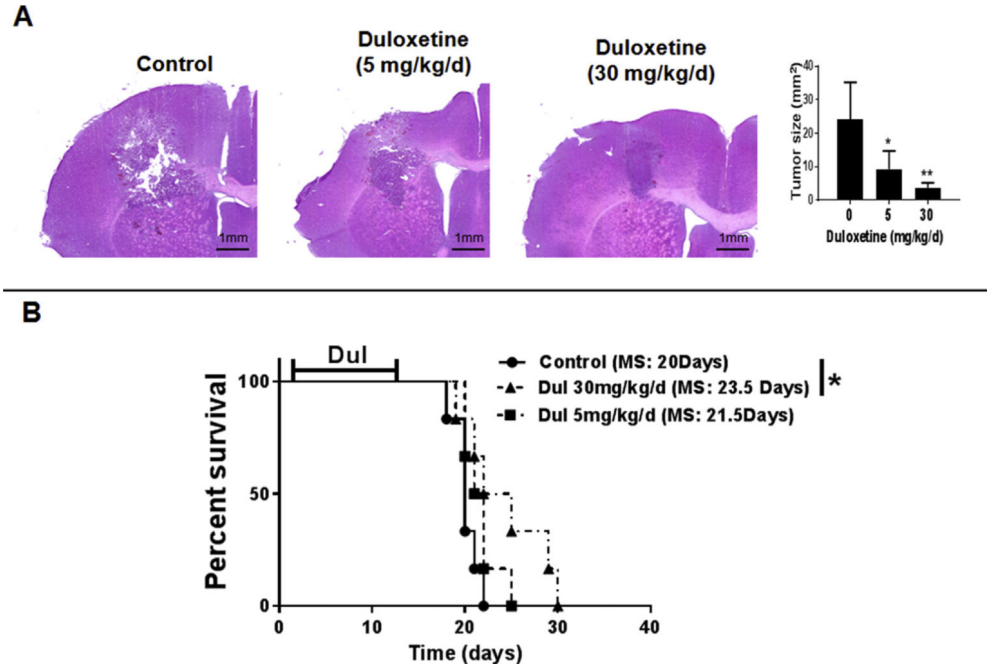

Fig. 4. Duloxetine (Dul) inhibited the growth of GL261 gliomas.

(A) Representative histology (left) and tumor volume measurements (right) demonstrating inhibition of i.c. GL261 tumor growth with Dul. Mice were treated with Dul a day after tumor implantation. Fourteen days later, brains were harvested and the largest tumor area was used for size calculations. (n =5 mice/group ± SD). **(B)** Kaplan–Meier survival curve of tumor-bearing mice treated with daily vehicle or Dul for 14 days (n = 6 mice/group). Animals demonstrating signs of elevated intracranial pressure were euthanized and tumor presence confirmed by histology. *: $p < 0.05$, **: $p < 0.01$ compared to control group. MS: median survival. Results are representative of two separate experiments.

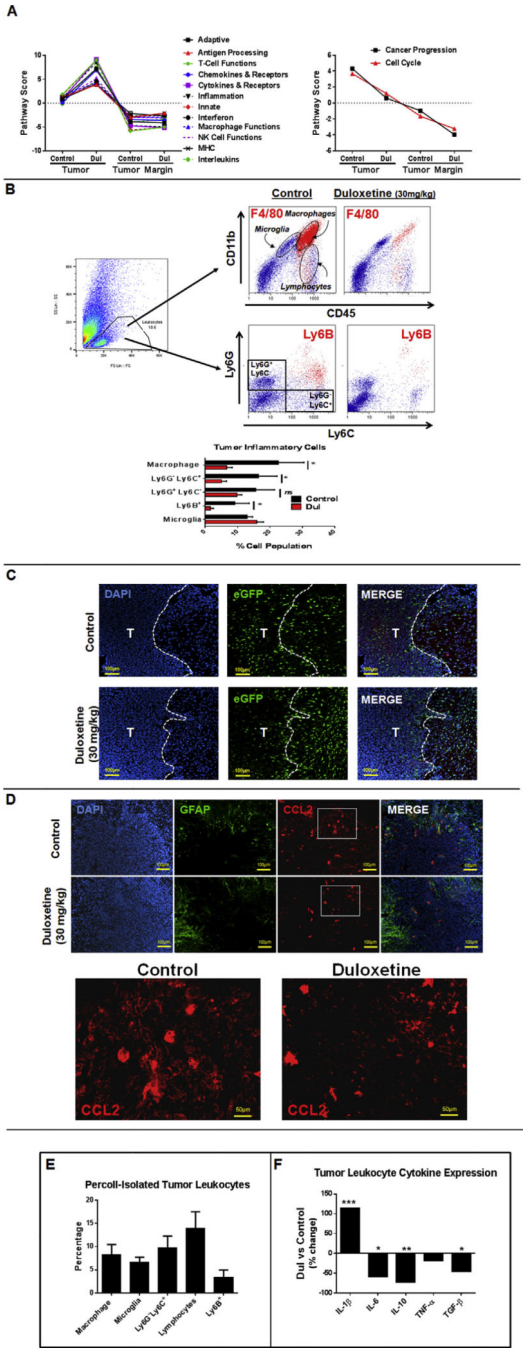

Fig. 5. Effect of duloxetine (Dul) on tumor inflammatory responses.

(A) To assess the overall inflammatory changes in tumor and tumor microenvironment (TME), tumors and peritumoral tissue from brains of control and Dul-treated GL261-bearing mice were dissected and analyzed by Nanostring. Pathway Scores for a number of inflammatory processes were elevated in Dul-treated tumors, but not TME. **(B)** Representative dot plots (upper panel) and FACS quantification (lower panel) demonstrating a decrease in the proportion of macrophages (i.e. $CD11b^{+}$ $CD45^{high}$ $F4/80^{+}$), monocytic myeloid-derived cells ($CD11b^{+}$ $Ly6G^{-}$ $Ly6G^{+}$) and neutrophils ($Ly6B^{+}$), but not microglia

(i.e. $CD11b^{+}$ $CD45^{low}$) following a two-week treatment with Dul (30 mg/kg x 14 days). n = 3 mice/group ± SD. *: $p < 0.05$. **(C)** Representative sections of tumor-bearing brains demonstrating distribution of microglia and macrophages ($eGFP^{+}$) into GL261 tumors (T) and tumor edge. $CX_3CR_1^{GFP}$ mice were implanted with GL261 cells and treated a day later with Dul (30 mg/kg) or vehicle for two weeks. Fewer $eGFP^{+}$ cells (myeloid-derived cells) were seen within the Dul-treated tumors **(D)**. Representative immunohistochemistry demonstrating decrease in CCL2 expression by tumors after Dul therapy. GFAP: glial fibrillary acidic protein (astrocyte marker). Lowest panel represents higher magnification of insets in the upper panel. **(E)** Inflammatory cells isolated from GL261 gliomas by Percoll separation mostly consisted of monocytic lineage (i.e. microglia, macrophages and monocytic myeloid-derived cells). **(F)** Effect of Dul on the cytokine expression profile of tumor-associate leukocytes. GL261 gliomas from vehicle or Dul-treated (30 mg/kg/14 days) mice were harvested at 14 days post tumor implantation and subjected to Percoll gradient. Leukocytes were isolated and incubated with LPS (0.5 μg/ml, 24 h). Cytokine expression was assessed by q-PCR. (n = 4 mice/group ± SD). Representative results from two separate experiments is shown.

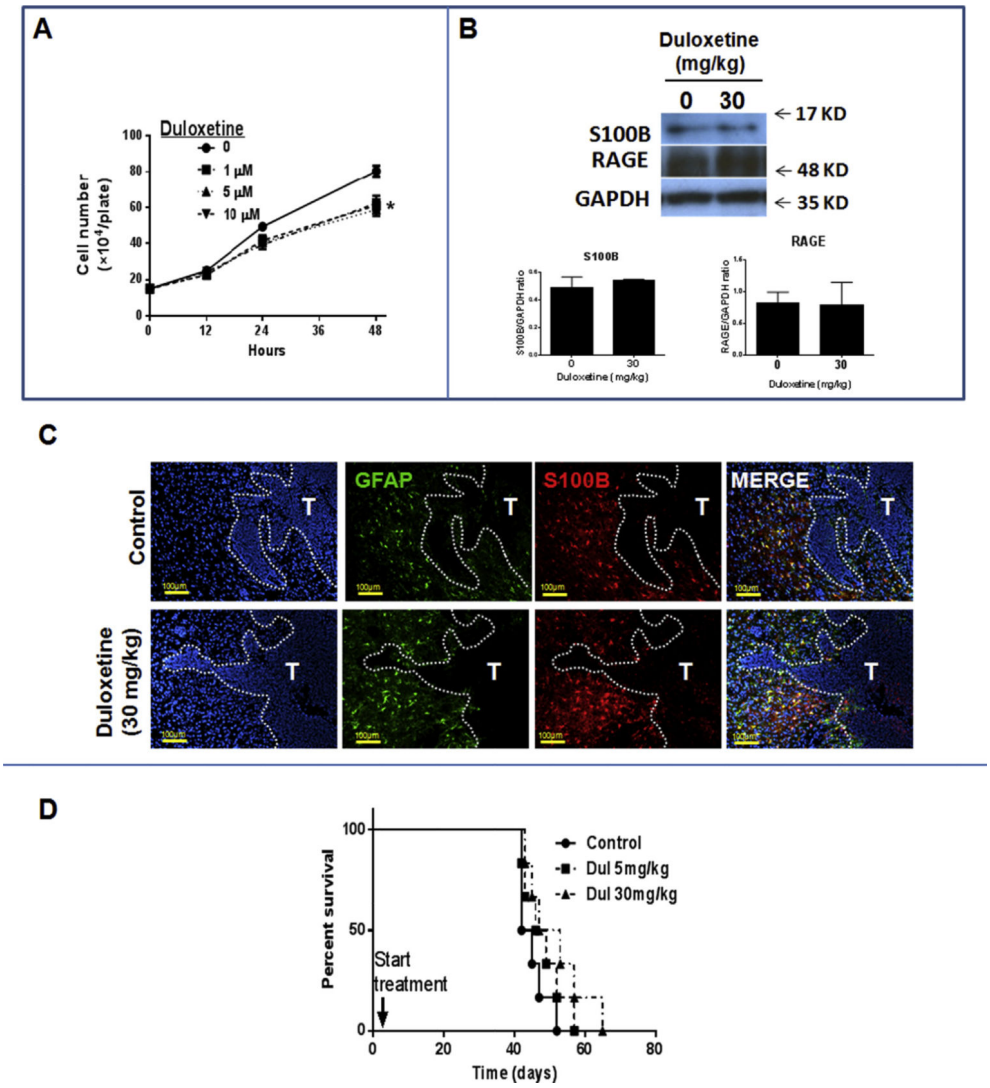

Fig. 6. ***In vitro*** **and** ***in vivo*** **activity of duloxetine (Dul) on K-Luc gliomas.**

(A) Dul inhibited K-Luc proliferation even at low concentrations. n = 3 ± SD. *: $p < 0.05$. **(B)** Dul did not inhibit brain S100B or RAGE protein levels in tumor-bearing animals. One day after K-Luc implantation, tumor-bearing mice were treated daily with Dul or vehicle. Fourteen days later, tumors and peritumoral tissue was harvested for protein analysis. (n = 3 mice/group ± SD). **(C)** Representative immunohistochemistry of i.c. K-Luc tumors (T) following a two-week treatment with Dul demonstrating persistent S100B expression by peritumoral astrocytes ($GFAP^+$ cells). **(D)** Dul did not inhibit K-Luc tumor growth. Tumor bearing mice were treated with daily vehicle or Dul for 14 days (n =6 mice/group). Animals demonstrating signs of elevated intracranial pressure were euthanized and tumor presence confirmed by histology. MS: median survival. Results are representative of two separate experiments.

Table 1

Duloxetine tissue and plasma concentration (μM).

Collection Time (hr)	GL261 Tumor	Brain Without Tumor	Plasma
0.5	48.79	36.30	3.04
2	70.84	65.87	2.12
6	24.85	24.22	1.28
12	10.04	9.64	0.39